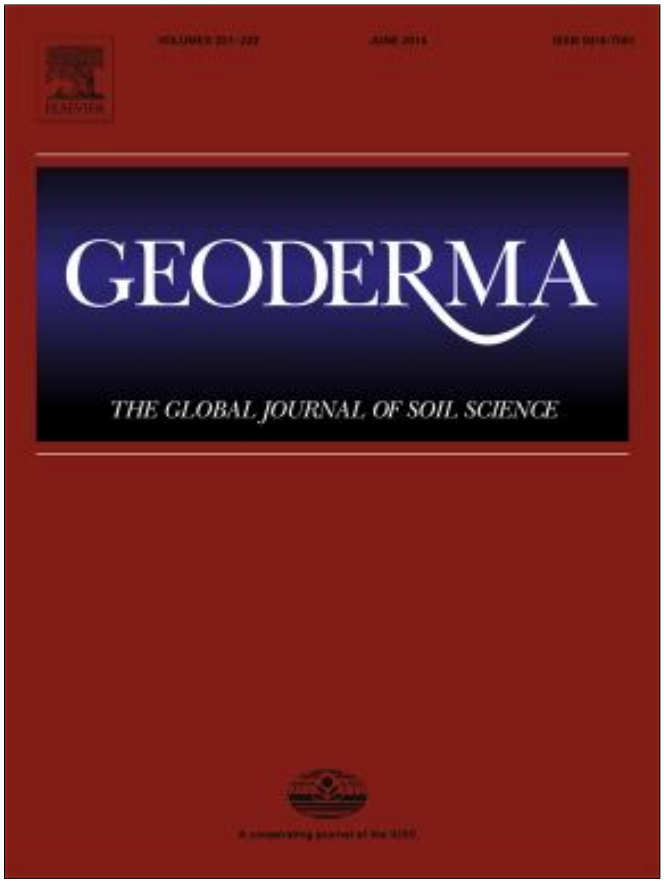

Geoderma 221–222 (2014) 139–145

Contents lists available at ScienceDirect

Geoderma

journal homepage: www.elsevier.com/locate/geoderma

Mobilization of colloidal carbon during iron reduction in basaltic soils

Shea W. Buettner [a], Marc G. Kramer [b], Oliver A. Chadwick [c], Aaron Thompson [a,*]

[a] Crop and Soil Sciences Department, University of Georgia, Athens, GA, USA
[b] Soil and Water Science Department, University of Florida, Gainesville, FL, USA
[c] Department of Geography, University of California, Santa Barbara, CA, USA

ARTICLE INFO

Article history:
Received 31 May 2013
Received in revised form 3 January 2014
Accepted 9 January 2014
Available online 7 February 2014

Keywords:
Hawaii
Soil organic matter
Anoxia
Iron reduction
pH
Asymmetric flow field-flow fractionation

ABSTRACT

The transport of organic carbon (C) to deep mineral horizons in soils can lead to long-term C stabilization. In basaltic soils, C associations with short-range-ordered (SRO) minerals often lead to colloid-sized aggregates that can be dispersed and mobilized by changes in soil solution chemistry. In the montane forest region of Hawaii, basaltic soils are exposed to high rainfall and anoxic conditions that facilitate ferric (Fe^{III}) (oxyhydr)oxide reduction. We explored the potential of iron (Fe)-reducing conditions to mobilize C by exposing the surface mineral horizons of three soils from the Island of Hawai'i (aged 0.3, 20, and 350 ky) to 21 days of anoxic incubation in 1:10 soil slurries. Mobilized C was quantified by fractionating the slurries into three particle-size classes (<430 nm,<60 nm,<2.3 nm ≈ 10 kDa). In all three soils, we found Fe reduction (maximum Fe^{2+} (aq) concentration ≈ 17.7 ± 1.9 mmol kg^{-1} soil) resulted in ~500% and ~700% increase of C in the 2.3–430 nm, and <2.3 nm size fractions, respectively. In addition, Fe reduction increased solution ionic strength by 127 μS cm^{-1} and generated hydroxyl ions sufficient to increase the slurry pH by one unit. We compared this to C mobilized from the slurries during a 2-h oxic incubation across a similar range of pH and ionic strength and found smaller amounts of dissolved (<2.3 nm) and colloidal (2.3–430 nm) C were mobilized relative to the Fe reduction treatments ($p < 0.05$). In particular, C associated with the largest particles (60–430 nm) was dispersed almost exclusively during the Fe reduction experiments, suggesting that it had been bound to Fe-oxide phases. Our experiments suggest that colloidal dispersion during Fe-reducing conditions mobilizes high concentrations of C, which may explain how C migrates to deep mineral horizons in redox dynamic soils.

1. Introduction

Earth's carbon (C) cycle is influenced by the distribution and behavior of C in soils. Considerable effort is now directed at understanding the mechanisms regulating soil C stabilization and turnover rates (Schmidt et al., 2011) as a function of climate, including temperature, rainfall, and soil saturation (Giardina and Ryan, 2000; Schuur et al., 2001; Townsend et al., 1997; Trumbore, 1997). Many studies observe C deep in the soil profile has longer turnover times than surface soil C (Harrison et al., 2011; Torn et al., 1997). These studies suggest a lower microbial activity and increased association with mineral surfaces—particularly short-range-ordered (SRO) minerals (Chorover et al., 2004; Kramer et al., 2012; Lalonde et al., 2012; Mikutta et al., 2009)—contribute to the persistence of C at depth. Photosynthetically fixed C deposited at the soil surface can be delivered to deep soil horizons directly by root death; indirectly by biological or physical mixing; or by advection with soil solution (Strahm et al., 2009). The advective transport of dissolved or colloidal C is greatly facilitated by preferential flow channels, which reduce the travel time and potential for degradation during transport.

Hawaiian rainforest ecosystems lose mobile organic C from surface horizons to deeper ones and to streams creating pathways for removal of organically bound nutrients from terrestrial ecosystems (Hedin et al., 2003; Neff et al., 2000; Vitousek, 2004). The volcanic soils in these forests are rich in SRO minerals, which along with their strong C sorption capabilities also are prone to shrinking and swelling depending on rainfall frequency. As a consequence, cracks between peds provide preferential flow paths that carry organic matter from O and Bh horizons to deeper horizons where they are sorbed on SRO minerals (Marin-Spiotta et al., 2011). Marin-Spiotta et al. (2011) suggest both dissolved and particulate C are important vehicles for C transport in these soils, but they report only soluble C and do not offer a mechanism for the generation of mobilized organic carbon (MOC). The soils studied by Marin-Spiotta et al. (2011) receive about 3000 mm rainfall annually and experience periods of episaturation and anoxia that promote Fe reduction and lead to a net loss of Fe from the upper horizons. Reductive dissolution of Fe^{III}-oxides can promote colloid dispersion by dissolving the connective Fe cement holding aggregates together (Goldberg and Glaubig, 1987). Also, because Fe reduction consumes protons and causes an increase in solution pH (Gillespie, 1920; Ponnamperuma et al., 1966; Vesparaskas and Faulkner, 2001), it can indirectly influence colloid dispersion through development of negative charge on colloid surfaces (Bunn et al., 2002; Ryan and Gschwend, 1994). Therefore, Fe

* Corresponding author. Tel.: +1 706 410 1293; fax: +1 706 542 0914.
E-mail address: AaronT@uga.edu (A. Thompson).

0016-7061/$ – see front matter © 2014 Elsevier B.V. All rights reserved.
http://dx.doi.org/10.1016/j.geoderma.2014.01.012

reduction can influence colloidal mobilization physically via dissolution of particles or chemically through changes in pH and corresponding particle surface charges (Thompson et al., 2006a). Fimmen et al. (2008) and Grybos et al. (2009) have suggested that organic matter is likely to disperse during Fe–C redox cycles, although they do not provide direct evidence of organic colloids.

Our research objective is to quantify changes in dissolved (<10 kDa), nanoparticulate (2.3–60 nm), and colloidal (60–430 nm) organic matter following Fe reduction events and induced pH increases. We use surface soils from Hawaiian rainforests and subject them to laboratory shifts in redox and pH to simulate conditions prevalent in these high-rainfall (>2500 mm/yr) ecosystems. We hypothesize that anoxic conditions destabilize C in organic-rich basaltic soils and generate mobile organic colloids. Thompson et al. (2006a) have shown that Fe reduction in similar-age Hawaiian soils promoted colloid dispersion primarily through the indirect effects of hydroxide production. We suspect that increases in pH associated with reduction reactions play a role in enhancing carbon release as well. To test these hypotheses, we measured the C content across three particle size classes following laboratory incubations of the soils exposed to either a 21-day period of anoxia or short-term pH adjustments.

2. Materials and methods

2.1. Site description

For this study, we selected surface mineral soil horizons from three sites on the Island of Hawai'i. The soils were collected in July 2009 from the Thurston (A horizon) and Laupāhoehoe (Ag/Bh horizon) sites reported in Kramer et al. (2012), and Pu'u Eke (Bh horizon) site reported in Marin-Spiotta et al. (2011). The Pu'u Eke soil (a Hydric Hapludand or Hydric Placudand) developed in the Pololu flows on Kohala Mountain, which are ca. 350 ka; the Laupāhoehoe soil (a Thaptic Udivitrand) formed in volcanic ejecta from Mauna Kea and is ca. 20 ka; and the Thurston soil (a Lithic Hapludand) lies on Kiluaea and formed in volcanic ejecta that is ca. 0.3 ka (Fig. 1). Detailed characteristics of these soils are provided elsewhere (Kramer et al., 2012; Marin-Spiotta et al., 2011). Although SRO abundance increases progressively with age across these soil profiles as a whole, the SRO content of these surface mineral horizons peaks at the Laupāhoehoe site and then decreases in the Pu'u Eke site (Table 1). Once collected, the soils were stored at 4 °C under oxic conditions in the dark until used in the May 2010 experiments.

2.2. Anoxic experiment

Triplicate incubations of field-moist surface mineral soil horizons were suspended in 2.0 mM KCl at a soil:solution ratio of 1:10 (dry mass equivalent) in 12-mL polypropylene tubes. Soil-dry mass was determined after drying a separate subsample for 24 h at 110 °C. The suspensions were shaken in 12-mL polypropylene vials for 2 h on a horizontal shaker (~120 revolutions per minute, rpm). Three, 1.5-mL aliquots were removed and subjected to differential centrifugation targeting <430 nm and <60 nm particle-size fractions, as well as an ultrafiltration step (10 kDa) targeting a <2.3 nm fraction. The 430 nm cutoff was designed to target select particles below 0.45 μm, which is the cutoff for dissolved organic carbon used in the literature. The 60 nm value was selected to approximate conservatively a cutoff between nanoparticles (defined as <100 nm) and colloids (defined >100 nm). The <2.3 nm was chosen to represent a truly dissolved (non-particle) size fraction. These aliquots provided a pre-reaction sample set. The remaining suspension was opened in an anoxic chamber (95% N_2, 5% H_2) and allowed to equilibrate for 16 h before resealing. Suspensions were then secured on an end-over-end shaker (8 rpm) inside the glovebox and reacted for 21 d at room temperature (~25 °C). We monitored Fe^{II} production in the aqueous phase and terminated the experiment once Fe^{II} production began to increase substantially. Storaging tropical soils at 4 °C has been recently shown to slow the recovery of Fe reducing organisms (Ginn et al., 2014) and that may have contributed to the slow emergence of aqueous Fe^{II}.

Following incubation, size-fractionated samples were isolated by differential centrifugation in an Eppendorf 5430 centrifuge with a F45-

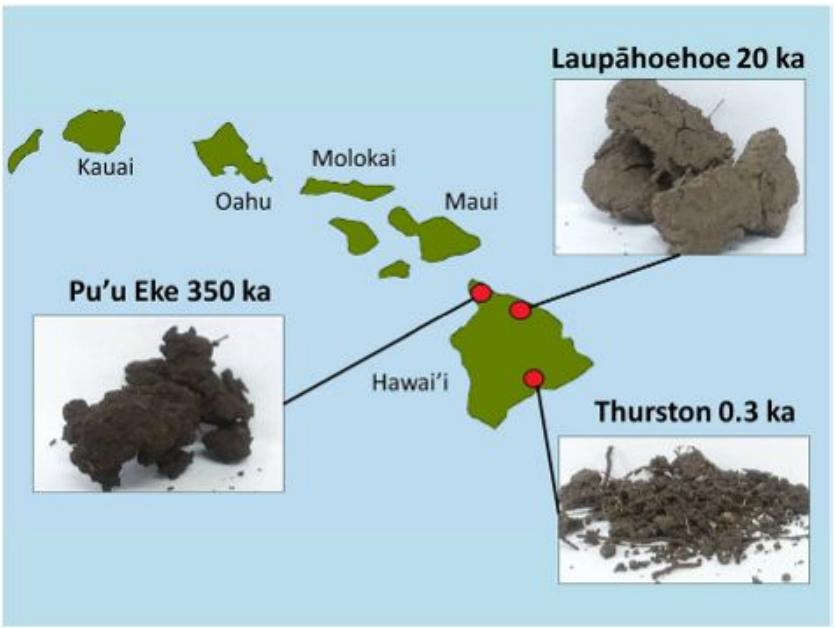

Fig. 1. Location of the experimental soils along with their approximate age and photo. All soils were collected from the volcanic Island of Hawai'i in July 2009. Thurston (A horizon) and Laupāhoehoe (Ag/Bh horizon) sites reported in Kramer et al. (2012), and Pu'u Eke (Bh horizon) site reported Marin-Spiotta et al. (2011). Pu'u Eke and Laupāhoehoe soils were visually more homogeneous and clayey than the Thurston soil (inset photos).

Table 1
Selected soil chemical data and site descriptions.

Soil[a]	Age (ky)	Horizon designation	Depth (cm)	C(%)[b]	SRO minerals (%)[c]	Native pH[d]
Thurston	0.3	A	10–18	8.4	9	6.0
Laupāhoehoe	20	Ag or Bh	12–20	32.8	14	3.6
Pu'u Eke[e]	350	Bh	15–25	22.1	1	4.2

[a] Values from Kramer et al. (2012), unless otherwise noted.
[b] Organic carbon content.
[c] Short-range-ordered Fe, Si, and Al; determined by the acid ammonium oxalate method.
[d] From Chorover et al. (2004) for the 0.3 and 20 ky soils and from Marin-Spiotta et al. (2011) for the Pu'u Eke soil.
[e] This soil is labeled Pololu in Kramer et al. (2012).

30-11 rotor for <430 nm and <60 nm hydrodynamic diameters. Centrifugal fractionation was achieved assuming spherical particle geometry and a nominal particle density of 1.65 g cm^{-3}. This was based on density separations (not shown) that indicated qualitatively that this was the median of particle mass. We assessed this assumption quantitatively for the Pu'u Eke soil (see Sec. 2.5), which has high organic matter content (Marin-Spiotta et al., 2011) and likely the lowest density among the samples.

The RCF and time required to achieve separation of particles <430 nm (3 min at 3195 RCF or 5400 rpm for 3 min), <60 nm (24 min at 21,169 RCF or 13,900 rpm for 24 min) was calculated from Stokes' law (Henderson et al., 2012). Samples were returned to the glovebox where the supernatant solutions were removed and acidified to pH 1 with trace metal grade 6 M HCl (0.8% of sample volume). The <2.3 nm fraction was obtained by centrifuging in a manner identical to the <60 nm fraction, and in the final step the supernatant was passed through a 10 kDa molecular weight cutoff Millipore Amicon-Microcon filter (at 14,000 rpm for 10 min) using an Eppendorf Minispin Plus centrifuge inside the glovebox. Prior to use, we removed glycerin contamination of the <10 kDa filters by running a solution of 0.1 M NaOH through the filters three times, followed by three 18.2 MΩ water washes. Filters were then immediately used for ultrafiltration of the soil solutions. The remaining C from the filters contributed less than 15 mg L^{-1} (~0.2 g kg^{-1} soil based on our standard dilution ratio; data not shown) to the filtrate and this C was accounted for through blank-subtraction.

2.3. Oxic pH shifted experiment

A separate experiment was conducted under oxic conditions to isolate the effects of pH on colloidal C mobilization. The intent of the oxic pH shifted experiments was to quantify colloidal dispersion in the anoxic incubations resulting solely from the development of negative particle surface charge associated with the higher slurry pH following Fe reduction. Thus, we adjusted the slurry electrical conductivity (EC) and pH to span the conditions of our anoxic experiments and confirm statistically similar EC values. The suspensions were equilibrated between 3 and 5 mM ionic strength across a pH range of 4 to 6 through measured additions of 0.1 M KOH. The suspensions were then shaken on a horizontal shaker for 2 h and sampled following procedures described previously for the anoxic samples (e.g., differential centrifugation and ultrafiltration).

2.4. Sample analysis

We measured pre- and post-experimental pH, EC, and redox potential (Eh) data on both the anoxic and pH shifted oxic treatments. Organic carbon (TOC) in the aqueous and solid phases was analyzed by high-temperature combustion following sparging of acidified samples on a Shimadzu TOC-5050A with Shimadzu ASI-500 sampler. To access the presence of reducing conditions in the anoxic experiment, we measured ferrous iron using a revised ferrozine spectrophotometric method given in Thompson et al. (2006b)) on a Shimadzu UV-1700 Spectrophotometer. We utilized Excel Stat (a Microsoft Excel plug-in) for statistical analysis. Incubation TOC concentrations were subjected to a Tukey's HSD test for post-ANOVA pair-wise comparisons in a one-way ANOVA.

2.5. Multi-angle light scattering and AF4 analysis

Particle size of our Pu'u Eke separations was validated on an Eclipse 2 (Wyatt Technology) asymmetric flow field-flow fractionation (AF4) channel (19.7 cm × 5.6 cm) coupled to a DAWN Heleos® multi-angle laser light scattering (MALS) device (Wyatt Technology). The AF4 separates particles on the basis of their diffusion coefficients in a flow channel. The AF4 was operated with a 490 μm thick separation spacer and a 10 kDa cellulose membrane. Our carrier solution was MES-SDS buffer (pH 6) prepared from 18.2 MΩ H2O with 0.3 mM sodium dodecyl sulfate and 2 mM of MES with 200 mg L^{-1} sodium azide to prevent bacterial growth. Particle separation of the samples was done by loading 30 μL of the solution into the AF4 via the injection loop on the Eclipse 2. The channel flow was kept constant at 1.0 mL min^{-1} channel flow, while the crossflow was set on gradient from 0.5 mL min^{-1} to zero over 25 min with an initial 6 minute time lapse for sample injection and focusing during which a focus flow set at 1.5 mL min^{-1} was operational. The total run time was 40 min per sample. Light-scattering data were collected simultaneously at 18 scattering angles on each eluting sample, subjected to real time digital correlation analysis on a Quasi-Elastic Light Scattering device (Wyatt-QELS) and analyzed for hydrodynamic radius using the Astra® instrument software (Dubascoux et al., 2008).

3. Results

3.1. Anoxic experiment

The initial pH of the soil slurries (Table 2) was similar to prior pH measurements of these surface soils (Chorover et al., 2004; Mikutta et al., 2009). Following the 21-day anoxic incubation, all soil slurries exhibited increases in pH, EC, aqueous [Fe^{+2}], and a decrease in Eh (Table 2). The pH increase was similar between the Laupāhoehoe (20 ka) and Pu'u Eke (350 ka) soils (~0.7 pH units; $p < 0.05$, $p < 0.01$), while considerably greater (~1.6 units; $p < 0.01$) for the Thurston (0.3 ka) soil, likely reflecting differences in the pH range of the Thurston soil as the calculated soil buffering capacity (assuming a 2 mol H^+ are consumed per mole of Fe^{III} reduced to Fe^{2+}, see Table S-2 in Thompson et al., 2006a) was between 33 and 38 mmol C kg^{-1} for all soils. Likewise the lower Eh for the Thurston soil following the anoxic incubation is partially due to the higher pH of this soil with final Eh values adjusted to pH 7 (Bartlett and

Table 2
Solution data (<430 nm) from the 21-day anoxic experiment.

	Thurston	Laupāhoehoe	Pu'u Eke
Pre pH	4.79 ± 0.02	4.03 ± 0.3	3.92 ± 0.01
Pre EC (dS m^{-1})	0.32 ± 0.01	0.31 ± 0.03	0.43 ± 0.01
Pre Eh (mV)	349 ± 9	428 ± 26	418 ± 18
Post Fe^{+2} (mmol kg^{-1})	19 ± 3	17 ± 2	17 ± 1
Post pH	6.43 ± 0.03	4.64 ± 0.04	4.73 ± 0.04
Post EC (dS m^{-1})	0.56 ± 0.05	0.48 ± 0.05	0.51 ± 0.02
Post Eh (mV)	−348 ± 21	−319 ± 48	−254 ± 32
Total C (g kg^{-1})	7.1 ± 1.1	7.1 ± 0.9	5.2 ± 0.6

Values are mean ± SD.

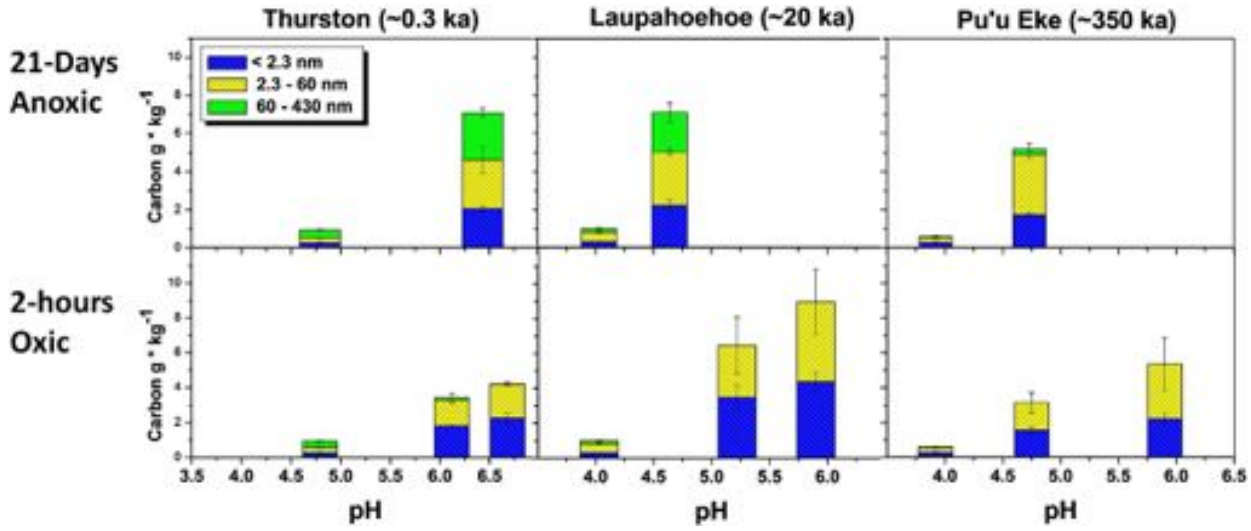

Fig. 2. Hawaiian soil (Thurston, Laupāhoehoe, Pu'u Eke) carbon size fraction concentrations (g C kg^{-1} soil) as related to pH in 21-day anoxic and 2-h oxic conditions in stacked bars. Blue bars with diagonal stripes (bottom bar) represent carbon less than 2.3 nm in diameter, yellow bars with cross-hatching (middle bar) represent carbon between 2.3 and 60 nm in diameter, and green bars with vertical stripes (top bar) represent carbon between 60 and 430 nm in diameter. Brackets indicate 1 standard deviation (n = 3).

James, 1993) of −348, −319 mV, and −254 mV for the 0.3 ky, 20 ky, and 350 ky soils, respectively.

At the beginning of the anoxic experiment, total carbon (<430 nm) desorbed from the soils was 0.93 ± 0.03 g kg^{-1}, 1.01 ± 0.05 g kg^{-1}, 0.61 ± 0.03 g kg^{-1} for the 0.3 ky, 20 ky, and 350 ky soils, respectively, with C distributed similarly across the three particle size fractions (Fig. 2). Following the anoxic incubation total desorbed C (<430 nm) increased ($p < 0.01$) to 7.1 ± 0.3 g kg^{-1}, 7.1 ± 0.5 g kg^{-1}, 5.2 ± 0.3 g kg^{-1} for the 0.3 ky, 20 ky, and 350 ky soils, respectively. The distribution of C across the three particle size fractions (<2.3 nm, 2.3–60 nm, and 60–430 nm) was similar before and after incubation across all soils, with the amount of C in each size fraction relatively similar in the 0.3 ky and 20 ky soils. However, the 350 ky soil contained less C in the 60–430 nm particle size class than the other two soils and this accounted for the majority of its lower total C desorption (Fig. 2).

3.2. Oxic pH shifted experiment

Total desorbed C (<430 nm) increased ($p < 0.01$) with increasing pH in the oxic experiments (Fig. 2), resulting in C release interpolated at the final pH of the anoxic experiments of 3.8 g kg^{-1}, 3.7 g kg^{-1}, 2.7 g kg^{-1} for the 0.3 ky, 20 ky, and 350 ky soils, respectively (Tables 2 and 3). In contrast with the anoxic incubations, increasing pH by addition of KOH under oxic conditions primarily dispersed C less than 60 nm, which was distributed similarly between the <2.3 nm and the 2.3–60 nm size fractions. In addition, if we interpolate the quantity of carbon that would be dispersed under oxic conditions (compared to anoxic incubations) we find the oxic incubations of all soils dispersed less C in the <2.3 and 2.3–60 nm size fractions, with the exception of the <2.3 nm size fraction of the Thurston soil ($p < 0.05$).

3.3. Nanoparticle characterization

The hydrodynamic radius of the oxic pH-shifted Pu'u Eke soil particles (<430 nm diameter) was validated by asymmetrical flow field-flow fractionation, AF4 (Fig. 4). It is apparent from the chromatogram that particle aggregation occurred as we documented significant amounts of smaller particles in our centrifugation separations, but these are not detectable in light-scattering system. Instead, it appears that the colloids did not elute from the channel until nearly zero cross flow rate was achieved, resulting in a band of 320–460 nm sized particles. The absence of smaller sized particles might be attributed to immobilization or loss into the membrane of the accumulation wall (Wahlund and Giddings, 1987) or more likely aggregation during the "focus" phase of the AF4 (Benincasa et al., 2002; Lead et al., 1997). Additionally, the lack of particle separation into bins of identical sizes "hides" the smaller particles among the larger during MALS analysis (Wyatt, 1998). However, this data does support our upper size cutoff for our centrifugations.

Table 3
Solution data (<430 nm) from the 2-h oxic experiment.

Soil (age)	pH	EC (dS m^{-1})	Eh (mV)	Fe^{+2} (mmol kg^{-1})	Interpolated Total C (g kg^{-1})
Thurston (0.3 ka)	4.79 ± 0.02	0.324 ± 0.029	349 ± 9	BD[a]	3.8 at pH 6.43
	6.12 ± 0.24	0.461 ± 0.025	457	BD	
	6.68 ± 0.30	0.471 ± 0.024	592	BD	
Laupāhoehoe (20 ka)	4.03 ± 0.30	0.310 ± 0.029	428 ± 26	BD	3.7 at pH 4.64
	5.22 ± 0.05	0.514 ± 0.025	515	BD	
	5.90 ± 0.06	0.551 ± 0.012	576	BD	
Pu'u Eke (350 ka)	3.92 ± 0.01	0.434 ± 0.029	418 ± 18	BD	2.7 at pH 4.73
	4.75 ± 0.09	0.453 ± 0.036	489	BD	
	5.90 ± 0.16	0.495 ± 0.009	584	BD	

Values are mean ± SD.
[a] BD, below detection limit ≈ 0.002 mmol kg^{-1}.

4. Discussion

4.1. Carbon mobilization during Fe reduction

The downward mobilization of colloidal organomineral complexes is an important process driving elevated SOM in volcanic subsoils (Osher et al., 2003). The onset of anoxic conditions in organic-rich soil horizons commonly triggers an increase in soil solution C (Fiedler and Kalbitz, 2003; Grybos et al., 2009; Hagedorn et al., 2000; Jacinthe et al., 2003; Kogel-Knabner et al., 2010; MacDonald et al., 2011). While lower C mineralization rates via anaerobic vs. aerobic metabolism may play a role (Fiedler and Kalbitz, 2003; Kalbitz et al., 2000; Moore and Dalva, 2001), most studies ascribe this increase in DOC to reduction-driven loss of Fe-(oxyhydr)oxide surface area for C sorption (e.g., Kogel-Knabner et al., 2010). Consistent with this paradigm all of our soils released more C during the anoxic incubations than at similar pH in oxic incubations ($p < 0.01$; Table 2). In addition, our incubations release six to over 400 times as much carbon during anoxic incubation than previously published work (Fiedler and Kalbitz, 2003; Grybos et al., 2009; Hagedorn et al., 2000; Jacinthe et al., 2003; MacDonald et al., 2011). The high amounts of C mobilization in our study likely reflect the substantial (8–32%) C content of the horizons we studied, although C content does not explain the slightly lower dispersion of C in the Pu'u Eke (350 ky) soil relative to the other soils (Tables 1 and 2).

Our work suggests that nanoparticulate and colloidal C are important contributors to mobile organic carbon (MOC), which have been overlooked in previous studies that lump DOC as any C that passes through 200 nm (e.g., Grybos et al., 2009), 450 nm (e.g., Fiedler and Kalbitz, 2003; Hagedorn et al., 2000; MacDonald et al., 2011), or even micron sized filters (e.g., Jacinthe et al., 2003). In fact, the large majority of MOC released in our anoxic experiment was colloidal (<430 nm) or nano-particulate C (2.3–60 nm) rather than soluble C (<10,000 Da) (Figs. 2 and 3). Mobilization of colloidal and nano-particulate C during Fe reduction likely occurs because of dissolution of an Fe-oxide matrix (Henderson et al., 2012; Ryan and Gschwend, 1992), or because the increase in pH accompanying Fe reduction generates negative particle surface charge and hence dispersion (Thompson et al., 2006a). Our experiments suggest both mechanisms contribute to colloid mobilization (Section 4.2) with important implications for soil C dynamics (Section 4.3).

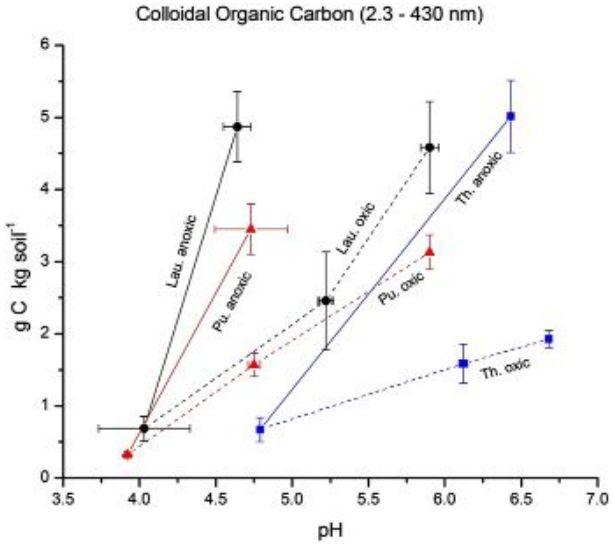

Fig. 3. Hawaiian soil (Thurston (Th.), Laupāhoehoe (Lau.), Pu'u Eke (Pu.)) colloidal (2.3 nm–430 nm) carbon concentrations (g C kg^{-1} soil) as related to pH in 21-day anoxic and 2-h oxic conditions. Solid lines represent anoxic experiments, while dashed lines are the oxic runs. Brackets indicate 1 standard deviation ($n = 3$).

4.2. Mechanisms of colloidal carbon mobilization

The mechanisms governing dispersion of soil colloids with increasing pH are well studied. As pH increases above the colloid point of zero charge (p.z.c.) hydroxyl functional groups deprotonate and generate repulsive electrostatic forces that disperse the particles. In many highly weathered soils, organic matter coatings on mineral colloids dominate the surface charge characteristics, poising the soil p.z.c. below pH 4 (Chorover and Sposito, 1995). This is especially true for most Hawaiian soils, which are replete with nanoscale organo-mineral phases containing a high density of ionizable surface functional groups (Chorover et al., 2004; Krishnaswamy and Richter, 2002; Mikutta et al., 2009; Osher et al., 2003). Fe reduction reactions consume protons following the general reaction (Ponnamperuma et al., 1966):

$$Fe(OH)_3 + e^- + 3H^+ \leftrightarrow Fe^{2+}(aq) + 3H_2O \quad (1)$$

Hence, development of Fe reducing conditions in acidic to neutral soils is nearly always accompanied by an increase in pH (Kirk, 2004). Several recent studies have illustrated the mobilization of organic matter in response to increases in pH (Grybos et al., 2007, 2009,) with some documenting colloidal forms of organic matter (Pédrot et al., 2008, 2009, 2011; Thompson et al., 2006a). We found that increasing the pH of all three of our Hawaiian soils through addition of KOH resulted in greater release of nanoparticulate (2.3–60 nm) and dissolved C, but the amount of colloid-bound (60–430 nm) C was minimally affected (Fig. 2). In contrast, our anoxic experiments, in which Fe reduction drove a similar pH increase, yielded 60% more nanoparticulate and colloidal (non-dissolved) C than was released from oxic samples at similar ionic strength and pH ($p < 0.01$; Fig. 3). Not only did the nanoparticles (2.3–60 nm) exhibit uniformly higher C contents following Fe reduction than after oxic incubation at equivalent pH ($p < 0.05$), but in Thurston (0.3 ka) and Laupāhoehoe (20 ka) soils Fe reduction dispersed substantially more 60–430 nm particulate C than the oxic incubations at an equivalent pH (Fig. 2). Very little 60–430 nm particulate C was dispersed in the Pu'u Eke (350 ka) soil in either anoxic or oxic incubations (Fig. 2). Those particles may simply be less abundant in this soil, or perhaps the lower SRO mineral abundance has some impact (Table 1).

Iron minerals are common binding agents for larger soil aggregates (Arduino et al., 1989), especially the high surface area, nanoparticulate and SRO Fe phases that are most susceptible to reductive dissolution (Bonneville et al., 2004). Reducing conditions can dissolve these Fe-oxide coatings that bind colloids into larger aggregates and facilitate particle dispersion (Ryan and Gschwend, 1992). In fact, De-Campos et al. (2009) have shown Fe reduction decreases soil macro-aggregate stability to a greater extent than changes in solution pH alone. Our work suggests this disaggregation via reductive Fe dissolution also drives the dispersion of <430 nm C-containing particles (Fig. 4). Importantly, the combination of Fe reduction and an increase in pH perturbs larger colloidal C (60–430 nm) whereas this size range remains largely undispersed when subjected to pH increases alone.

4.3. Implications of anoxia on carbon mobilization

Regardless of the mechanism, the composition of C mobilized in colloidal form is not constrained by the need for aqueous solvation. This constraint biases typical DOM toward low molecular weight organic matter with abundant polar functional groups (i.e., hydroxyls). Instead, colloid-bound mobile organic matter may exhibit a wider range of characteristics including non-polar or aliphatic-rich materials that have low solubility as well as carboxylic-acid-rich materials that are strongly associated with metal-oxide surfaces. This can have substantial implications for the stabilization of C in soils. Hawaiian soils are rich in

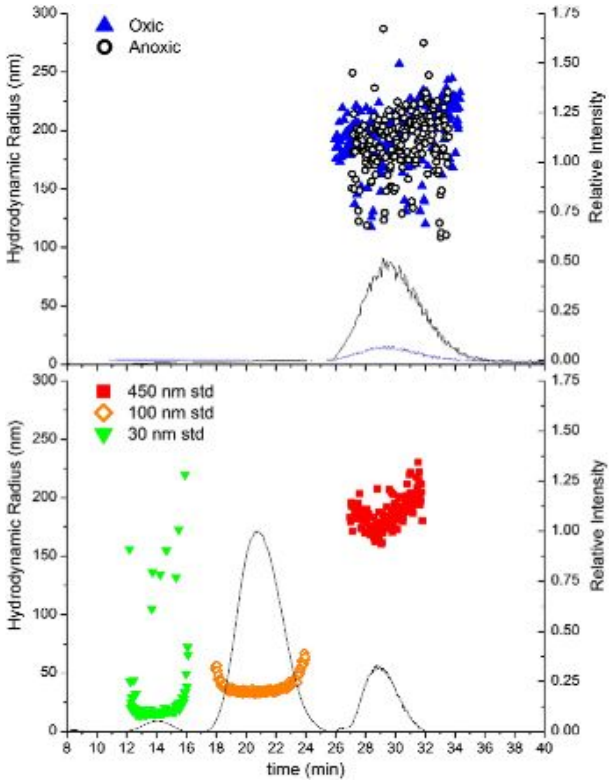

Fig. 4. Asymmetrical flow field-flow fractionation (AF4) data of <430 nm Pu'u Eke and a 30 (closed, point-down triangle), 100 (open diamond), and 450 (closed square) nm diameter standard. Solid lines represent relative intensity, while symbols represent particle hydrodynamic radius. The Pu'u Eke particles(upper graph) were below 230 nm in radius (i.e., <460 nm diameter).

hydrated-SRO minerals that shrink in response to periodic droughts and generate cracks in subsurface B horizons (Marin-Spiotta et al., 2011). Carbon mobilization to depth in these basaltic soils is linked to preferential-flow pathways developing along these cracks and macropores in the higher rainfall regions (Lohse and Dietrich, 2005; Marin-Spiotta et al., 2011). The zone of the greatest mobile organic carbon (MOC) production in our study soils—the surface forest litter horizons—also contains large quantities of Fe and Al and is subjected to intermittent saturation associated with the high rainfall (2800 to 3500 mm) (Marin-Spiotta et al., 2011). At the Pu'u Eke site, SOM accumulates along the surfaces of cracks that reach as deep as 70 cm into the soil profile. The functional group chemistry (based on NMR) of the SOM accumulating at depth resembles the Fe and Al-rich MOC released from the surface humic mineral horizons (Bh), where the network of cracks and channels is first observable (Marin-Spiotta et al., 2011). This metal-rich material is more likely to be mobilized as colloids (Pédrot et al., 2009; Pokrovsky et al., 2010; Schijf and Zoll, 2011; Thompson et al., 2006a) than true DOC and we suggest periodic Fe reduction events and shifts in pH are important in such mobilization.

5. Conclusion

We have demonstrated that Fe reduction events can mobilize substantial quantities of dissolved (<2.3 nm) and colloidal carbon (2.3–430 nm) in 0.3–350 ky old basaltic surface soils. Approximately half of this effect could be attributable to the increase in pH accompanying Fe reduction. However, raising the pH dispersed primarily the smallest colloids (<60 nm), while Fe reduction was largely responsible for dispersion of larger colloids (60 nm–430 nm). Our results suggest that mobilization of C from the surface to the subsoil is driven in part by Fe-redox induced particle dispersion during periodic saturation events. Because colloidal C can exhibit a much wider range of composition than dissolved organic carbon (DOC), this mobilization pathway has important implications for understanding the processes responsible for redistribution of C within soil profiles and along flow paths feeding waterways.

Acknowledgments

We thank Russell Henderson and Nehru Mantripragada for their laboratory assistance. We thank John Seaman for providing assistantship funding to SWB through the United States Department of Energy (DOE Award Number DE-FC09-07SR22506) and Savannah River National Lab, Area Closure Projects. Research funding was provided to AT by the United States Department of Agriculture (USDA), AFRI (Grant # 2009-65107-05830), the National Science Foundation (NSF) Geobiology and Low-temperature Geochemistry (Award # EAR-1053470).

References

Arduino, E., Barberis, E., Boero, V., 1989. Iron oxides and particle aggregation in B horizons of some Italian soils. Geoderma 45 (3–4), 319–329.
Bartlett, R.J., James, B.R., 1993. Redox chemistry of soils. Adv. Agron. 50, 151–208.
Benincasa, M.-A., Cartoni, G., Imperia, N., 2002. Effects of ionic strength and electrolyte composition on the aggregation of fractionated humic substances studied by flow field-flow fractionation. J. Sep. Sci. 25 (7), 405–415.
Bonneville, S., Van Cappellen, P., Behrend, T., 2004. Microbial reduction of iron(III) oxyhydroxides: effects of mineral solubility and availability. Chem. Geol. 212, 255–268.
Bunn, R.A., Magelky, R.D., Ryan, J.N., Elimelech, M., 2002. Mobilization of natural colloids from an iron oxide-coated sand aquifer: effect of pH and ionic strength. Environ. Sci. Technol. 36 (3), 314–322.
Chorover, J., Sposito, G., 1995. Colloid chemistry of kaolinitic tropical soils. Soil Sci. Soc. Am. J. 59 (6), 1558–1564.
Chorover, J., Amistadi, M.K., Chadwick, O.A., 2004. Surface charge evolution of mineral-organic complexes during pedogenesis in Hawaiian basalt. Geochim. Cosmochim. Acta 68 (23), 4859–4876.
De-Campos, A.B., Mamedov, A.I., Huang, C.H., 2009. Short-term reducing conditions decrease soil aggregation. Soil Sci. Soc. Am. J. 73, 550–559.
Dubascoux, S., Von Der Krammer, F., Le Hécho, I., Gautier, M.P., Lespes, G., 2008. Optimisation of asymmetrical flow field flow fractionation for environmental nanoparticles separation. J. Chromatogr. A 1206 (2), 160–165.
Fiedler, S., Kalbitz, K., 2003. Concentrations and properties of dissolved organic matter in forest soils as affected by the redox regime. Soil Sci. 168 (11), 793–801.
Fimmen, R., Richter, D., Vasudevan, D., Williams, M., West, L., 2008. Rhizogenic Fe–C redox cycling: a hypothetical biogeochemical mechanism that drives crustal weathering in upland soils. Biogeochemistry 87, 127.
Giardina, C.P., Ryan, M.G., 2000. Evidence that decomposition rates of organic carbon in mineral soil do not vary with temperature. Nature 404 (6780), 858–861.
Gillespie, L.J., 1920. Reduction potentials of bacterial cultures and water-logged soils. Soil Sci. 9, 199–216.
Ginn, B.R., Habteselassie, M.Y., Meile, C., Thompson, A., 2014. Effects of sample storage on microbial Fe-reduction in tropical rainforest soils. Soil Biol. Biochem. 68, 44–51.
Goldberg, S., Glaubig, R.A., 1987. Effect of saturating cation, pH, and aluminum and iron oxides on the flocculation of kaolinite and montmorillonite. Clay Clay Miner. 35, 220–227.
Grybos, M., Davranche, M., Gruau, G., Petitjean, P., 2007. Is trace metal release in wetland soils controlled by organic matter mobility or Fe-oxyhydroxides reduction? J. Colloid Interface Sci. 314, 490–501.
Grybos, M., Davranche, M., Gruau, G., Petitjean, P., Pédrot, M., 2009. Increasing pH drives organic matter solubilization from wetland soils under reducing conditions. Geoderma 154 (1–2), 13–19.
Hagedorn, F., Kaiser, K., Feyen, H., Schleppi, P., 2000. Effects of redox conditions and flow processes on the mobility of dissolved organic carbon and nitrogen in a forest soil. J. Environ. Qual. 29 (1), 288–297.
Harrison, R.B., Footen, P.W., Strahm, B.D., 2011. Deep soil horizons: contribution and importance to soil carbon pools and in assessing whole-ecosystem response to management and global change. For. Sci. 57 (1), 67–76.
Hedin, L.O., Vitousek, P.M., Matson, P.A., 2003. Nutrient losses over four million years of tropical forest development. Ecology 84 (9), 2231–2255.
Henderson, R., Kabengi, N., Mantripragada, N., Cabrera, M., Hassan, S., Thompson, A., 2012. Anoxia-induced release of colloid and nanoparticle-bound phosphorus in grassland soils. Environ. Sci. Technol. 46, 11727–11734.
Jacinthe, P.A., Groffman, P.M., Gold, A.J., 2003. Dissolved organic carbon dynamics in a riparian aquifer: effects of hydrology and nitrate enrichment. J. Environ. Qual. 32 (4), 1365–1374.
Kalbitz, K., Solinger, S., Park, J.H., Michalzik, B., Matzner, E., 2000. Controls on the dynamics of dissolved organic matter in soils: a review. Soil Sci. 165 (4), 277–304.

Kirk, G., 2004. Reduction and oxidation. In: Kirk, G. (Ed.), The biogeochemistry of submerged soils. John Wiley & Sons, Ltd., West Sussex, England, pp. 93–134.
Kogel-Knabner, I., Amelung, W., Cao, Z.H., Fiedler, S., Frenzel, P., Jahn, R., Kalbitz, K., Kolbl, A., Schloter, M., 2010. Biogeochemistry of paddy soils. Geoderma 157 (1–2), 1–14.
Kramer, M.G., Sanderman, J., Chadwick, O.A., Chorover, J., Vitousek, P.M., 2012. Long-term carbon storage through retention of dissolved aromatic acids by reactive particles in soil. Glob. Chang. Biol. 18 (8), 2594–2605.
Krishnaswamy, J., Richter, D.D., 2002. Properties of advanced weathering-stage soils in tropical forests and pastures. Soil Sci. Soc. Am. J. 66, 244–253.
Lalonde, K., Mucci, A., Ouellet, A., Gelinas, Y., 2012. Preservation of organic matter in sediments promoted by iron. Nature 483 (7388), 198–200.
Lead, J.R., Davison, W., Hamilton-Taylor, J., Buffle, J., 1997. Characterizing colloidal material in natural waters. Aquat. Geochem. 3 (3), 213–232.
Lohse, K.A., Dietrich, W.E., 2005. Contrasting effects of soil development on hydrological properties and flow paths. Water Resour. Res. 41.
MacDonald, J.D., Chantigny, M.H., Angers, D.A., Rochette, P., Royer, I., Gasser, M.O., 2011. Soil soluble carbon dynamics of manured and unmanured grasslands following chemical kill and ploughing. Geoderma 164 (1–2), 64–72.
Marin-Spiotta, E., Chadwick, O.A., Kramer, M., Carbone, M.S., 2011. Carbon delivery to deep mineral horizons in Hawaiian rain forest soils. J. Geophys. Res. 116 (G3), G03011.
Mikutta, R., Schaumann, G.E., Gildemeister, D., Bonneville, S., Kramer, M.G., Chorover, J., Chadwick, O.A., Guggenberger, G., 2009. Biogeochemistry of mineral-organic associations across a long-term mineralogical soil gradient (0.3–4100 kyr), Hawaiian Islands. Geochim. Cosmochim. Acta 73 (7), 2034–2060.
Moore, T.R., Dalva, M., 2001. Some controls on the release of dissolved organic carbon by plant tissues and soils. Soil Sci. 166 (1), 38–47.
Neff, J.C., Hobbie, S.E., Vitousek, P.M., 2000. Nutrient and mineralogical control on dissolved organic C, N and P fluxes and stoichiometry in Hawaiian soils. Biogeochemistry 51 (3), 283–302.
Osher, L.J., Matson, P.A., Amundson, R., 2003. Effect of land use change on soil carbon in Hawaii. Biogeosciences 65 (2), 213–232.
Pédrot, M., Dia, A., Davranche, M., Bouhnik-Lacoz, M., Henin, O., Gruaua, G., 2008. Insights into colloid-mediated trace element release at the soil/water interface. J. Colloid Interface Sci. 325, 187–197.
Pédrot, M., Dia, A., Davranche, M., 2009. Double pH control on humic substance-borne trace elements distribution in soil waters as inferred from ultrafiltration. J. Colloid Interface Sci. 339 (2), 390–403.
Pédrot, M., Le Boudec, A., Davranche, M., Dia, A., Henin, O., 2011. How does organic matter constrain the nature, size and availability of Fe nanoparticles for biological reduction? J. Colloid Interface Sci. 359 (1), 75–85.
Pokrovsky, O.S., Viers, J., Shirokova, L.S., Shevchenko, V.P., Filipov, A.S., Dupre, B., 2010. Dissolved, suspended, and colloidal fluxes of organic carbon, major and trace elements in the Severnaya Dvina River and its tributary. Chem. Geol. 273 (1–2), 136–149.
Ponnamperuma, F.N., Martinez, E., Loy, T., 1966. Influence of redox potential and partial pressure of carbon dioxide on pH values and the suspension effect of flooded soils. Soil Sci. 101 (6), 421–431.
Ryan, J.N., Gschwend, P.M., 1992. Effect of iron diagenesis on the transport of colloidal clay in an unconfined sand aquifer. Geochim. Cosmochim. Acta 56, 1507–1521.
Ryan, J.N., Gschwend, P.M., 1994. Effect of solution chemistry on clay colloid release from an iron oxide-coated aquifer sand. Environ. Sci. Technol. 28 (9), 1717–1726.
Schijf, J., Zoll, A.M., 2011. When dissolved is not truly dissolved—the importance of colloids in studies of metal sorption on organic matter. J. Colloid Interface Sci. 361 (1), 137–147.
Schmidt, M.W.I., Torn, M.S., Abiven, S., Dittmar, T., Guggenberger, G., Janssens, I.A., Kleber, M., Kogel-Knabner, I., Lehmann, J., Manning, D.A.C., Nannipieri, P., Rasse, D.P., Weiner, S., Trumbore, S.E., 2011. Persistence of soil organic matter as an ecosystem property. Nature 478 (7367), 49–56.
Schuur, E.A.G., Chadwick, O.A., Matson, P.A., 2001. Carbon cycling and soil carbon storage in mesic to wet Hawaiian montane forests. Ecology 82 (11), 3182–3196.
Strahm, B.D., Harrison, R.B., Terry, T.A., Harrington, T.B., Adams, A.B., Footen, P.W., 2009. Changes in dissolved organic matter with depth suggest the potential for postharvest organic matter retention to increase subsurface soil carbon pools. For. Ecol. Manag. 258, 2347–2352.
Thompson, A., Chadwick, O.A., Boman, S., Chorover, J., 2006a. Colloid mobilization during soil iron redox oscillations. Environ. Sci. Technol. 40 (18), 5743–5749.
Thompson, A., Chadwick, O.A., Rancourt, D.G., Chorover, J., 2006b. Iron-oxide crystallinity increases during soil redox oscillations. Geochim. Cosmochim. Acta 70 (7), 1710–1727.
Torn, M.S., Trumbore, S.E., Chadwick, O.A., Vitousek, P.M., Hendricks, D.M., 1997. Mineral control of soil organic carbon storage and turnover. Nature 389 (6647), 170–173.
Townsend, A.R., Vitousek, P.M., Desmarais, D.J., Tharpe, A., 1997. Soil carbon pool structure and temperature sensitivity inferred using CO_2 and $^{13}CO_2$ incubation fluxes from five Hawaiian soils. Biogeochemistry 38 (1), 1–17.
Trumbore, S.E., 1997. Potential responses of soil organic carbon to global environmental change. Proc. Natl. Acad. Sci. U. S. A. 94 (16), 8284–8291.
Vesparaskas, M.J., Faulkner, S.P., 2001. Redox chemistry of hydric soils. In: Richardson, J.L. (Ed.), Wetland Soils: Genesis, Hydrology, Landscapes, and Classification. CRC Press: Lewis Publishers, New York, pp. 85–105.
Vitousek, P.M., 2004. Nutrient Cycling and Limitation: Hawai'i as a Model System. Princeton Unversity Press, Princeton.
Wahlund, K.G., Giddings, J.C., 1987. Properties of an asymmetrical flow field-flow fractionation channel having one permeable wall. Anal. Chem. 59 (9), 1332–1339.
Wyatt, P.J., 1998. Submicrometer particle sizing by multiangle light scattering following fractionation. J. Colloid Interface Sci. 197 (1), 9–20.